



**HAL**  
open science

# A User Centric Blockage Model for Wireless Networks

François Baccelli, Bin Liu, Laurent Decreusefond, Rongfang Song

► **To cite this version:**

François Baccelli, Bin Liu, Laurent Decreusefond, Rongfang Song. A User Centric Blockage Model for Wireless Networks. IEEE Transactions on Wireless Communications, 2022, 21 (10), 10 p. 10.1109/TWC.2022.3166211 . hal-03646854

**HAL Id: hal-03646854**

**<https://hal.science/hal-03646854v1>**

Submitted on 5 Dec 2023

**HAL** is a multi-disciplinary open access archive for the deposit and dissemination of scientific research documents, whether they are published or not. The documents may come from teaching and research institutions in France or abroad, or from public or private research centers.

L'archive ouverte pluridisciplinaire **HAL**, est destinée au dépôt et à la diffusion de documents scientifiques de niveau recherche, publiés ou non, émanant des établissements d'enseignement et de recherche français ou étrangers, des laboratoires publics ou privés.

# A User Centric Blockage Model for Wireless Networks

François Baccelli<sup>†</sup>, Bin Liu<sup>†</sup>, Laurent Decreusefond, and Rongfang Song

**Abstract**—This paper proposes a cascade blockage model for analyzing the vision that a user has of a wireless network. This model, inspired by the classical multiplicative cascade models, has a radial structure meant to analyze blockages seen by the receiver at the origin in different angular sectors. The main novelty is that it is based on the geometry of obstacles and takes the joint blockage phenomenon into account. We show on a couple of simple instances that the Laplace transforms of total interference satisfies a functional equation that can be solved efficiently by an iterative scheme. This is used to analyze the coverage probability of the receiver and the effect of blockage correlation and penetration loss in both dense and sparse blockage environments. Furthermore, this model is used to investigate the effect of blockage correlation on user beamforming techniques. Another functional equation and its associated iterative algorithm are proposed to derive the coverage performance of the best beam selection in this context. In addition, the conditional coverage probability is also derived to evaluate the effect of beam switching. The results not only show that beam selection is quite efficient for multi-beam terminals, but also show how the correlation brought by blockages can be leveraged to accelerate beam sweeping and pairing.

**Index Terms**—Stochastic geometry, multiplicative cascade, blockage, beamforming, best beam selection, iterative algorithm, coverage probability

## I. INTRODUCTION

THE classical distance-based path-loss model with a separate shadowing term has been employed for decades in wireless network modeling. However, this simple model falls short in reflecting realistic blockage features where signals from multiple nearby transmitters are blocked by common obstacles, which leads to the correlated shadowing effect. Despite significant research efforts in this direction in the recent years, there is still a clear need for more accurate and yet tractable blockage/shadowing models, particularly so in the context of 5/6G beamforming.

### A. Prior Work

There is a vast literature on shadowing and the need for correlated shadowing. Reference [1] summarizes the state of the art on correlated shadowing models based on parametric path-loss functions of relative/absolute propagation distance and incidence angle. Reference [2] discusses the approach

This work was supported in part by ERC NEMO under the European Union’s Horizon 2020 research and innovation programme, grant agreement number 788851 to INRIA, by a Jiangsu Government Scholarship for Overseas Studies under Grant JS-2018-7, Jiangsu Provincial Department of Education, China. (Corresponding author: Bin Liu)

<sup>†</sup>François Baccelli and Bin Liu are co-first authors.

François Baccelli is with Ecole Normale Supérieure (ENS) and INRIA in Paris, France (email: Francois.Baccelli@ens.fr).

Bin Liu, Rongfang Song are with the School of Telecommunication and Information Engineering, Nanjing University of Posts and Telecommunications, China. (e-mail: {liubin0430, songrf}@njupt.edu.cn).

Laurent Decreusefond are with LTCI, Telecom Paris, I.P. Paris, France (e-mail: laurent.decreusefond@telecom-paristech.fr).

based on correlated log-normal shadowing random variable. All these prior models maintain the analytical tractability at the cost of missing the geometric features of blockages.

Another and more natural way to model correlated shadowing is based on stochastic geometry (SG) and more precisely on the use of random shape theory to represent the location and the shape of obstacles. Reference [3] surveys the state-of-art on SG based blockage models. This is used for both outdoor [4] and indoor [5] communications. These random blockage models achieve a good trade-off between tractability and accuracy, but fail in characterizing spatial correlation. In [6], a blockage model called the Manhattan-type urban model, leveraged Poisson line process to represent blockages. This model was expanded to 3-D indoor wireless environments [7] and outdoor planar networks [8]. These models allow one to take the joint blockage effect into account but are limited to cities/districts with a Manhattan-type structure.

Beamforming and directional transmission are central in 5G and 6G cellular networks. This is particularly true for mmWave frequencies where beamforming is used to compensate for the more severe path loss. This spurs research efforts on beam scanning, selection, pairing and switch performance evaluation in different blockage structures. Unfortunately, the vast majority of these works consider the independent blockage model [9] [10] or free space [11] [12] [13] [14] for tractability. They hence fall short in capturing the effect of correlated blockages on beamforming techniques. There is hence also a need for models allowing one to capture and analyze the effect of blockage correlation on beamforming techniques.

### B. Challenges and Contribution

The first part of this paper presents a correlated blockage model based on a Multiplicative Cascade (MC) model. Such cascades have been successfully used to describe nonlinear phenomena of multiplicative nature in signal processing [16], network traffic [17] etc. for many years. To the best of our knowledge, this is the first attempt to model correlated blockages in wireless networks using such tools. This cascade blockage model is parametric and can be used to represent several types of urban/suburb/rural scenarios, such as city centers, residential districts, business centers, suburban areas, etc. It is shown that instead of a representation in terms of integral forms as in classical SG models, the Laplace transform of interference can be obtained by iterative algorithms derived from the cascade functional equation. This is then used to derive the downlink coverage probability.

The second part of the paper is focused on the impact of blockage correlation on beamforming. The cascade is again used to establish a functional equation for the joint Laplace transform of interference in all angular sectors. This again leads to iterative algorithms which can be used to obtain the

coverage performance of the best beam selection scheme. We also analyze the conditional coverage probability in case of a beam switch. We illustrate the practical use of this in the context of beam scanning and pairing.

The main contributions of this paper can be summarized as follows:

1) A basic cascade model and two extensions are proposed to describe blockage environments. These models capture blockage correlation effects. Compared with independent models used in prior work, our models are equally tractable and more realistic. They also show that the independent blockage models underestimate the overall system performance.

2) For omnidirectional User Equipment (UE), new functional equations and iterative algorithms are proposed to derive Laplace transforms of total interference.

3) A beamforming capable UE can sweep the beamforming directions and choose the beam with the maximal Signal to Interference Ratio (SIR) as its serving beam. The blockage correlation complicates the computation of the best beam. We propose another functional equation and its associated iterative algorithm. This allows one to obtain the coverage probability in this case.

4) We leverage the cascade model to derive the conditional coverage probability after a beam switch. The analysis shows how to scan beams from a reference beam in order to shorten the beam scanning duration.

5) Simulation results validate the accuracy of analysis and are used to gain further insights on the impact of blockage correlation on coverage performance for both omnidirectional and beamforming UEs.

### C. Organization and Notation

The rest of paper is organized as follows. Section II introduces the system model. In Section III, we propose the iterative algorithm allowing one to evaluate coverage performance for omnidirectional UEs. Two variants of the basic cascade model of Section II allowing one to represent other blockage environments are discussed in Section IV. In Section V, we introduce the problem of the best beam selection and beam switch in correlated blockages. This is based on an analysis of the joint distribution of interference in different angular sectors. An algorithm to compute this joint distribution is also give. This is the basis of the evaluation of coverage probability of the best beam policy when users have beamforming functionalities. Beam switching performance is further evaluated in Section VI. Finally, we conclude the paper in Section VII. Table I gathers the notation used throughout.

## II. SYSTEM MODEL

In a cellular network, the transmission between BSs and users are often blocked by obstacles like buildings, cars and walls. In most cities, towns or districts, blockages have the following basic physical features: *Firstly*, their locations are often aligned along with certain geometric objects such as avenues, streets, roads, and rivers thanks to urban planning. *Secondly*, most blockages are not as regular as those in

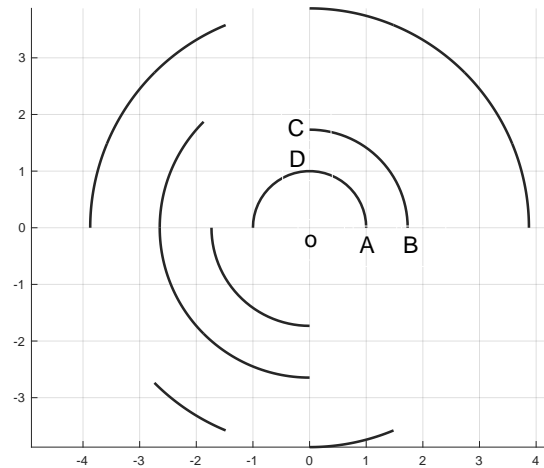


Fig. 1: An example of basic cascade blockage model. The origin represents typical user and the solid curves are blockages.

Manhattan-type cities. *Thirdly*, the nearer the blockage, the larger the angle with which a given user sees it.

Consider BSs deployed uniformly on the plane and a typical user located at the origin. Assume obstacles hindering electromagnetic propagation to be also deployed in the plane. These obstacles can have very different structures depending on the environment (urban/suburb/rural areas). For example, buildings are organized in dense and locally periodic structures in urban areas, whereas they may have a sparse and random structure in rural areas. These features are partially captured by the following radial model.

### A. The Basic Radial Blockage Model

A cascade is an iterative procedure that divides a given set into smaller and smaller sets using some subdivision rules [16] [17]. In the proposed model, the blockages are created according to a cascade procedure operated on some angular domain, e.g.,  $[0, 2\pi]$  if the antenna of the receiver is omnidirectional. In the proposed model, the blockages are arranged as a collection of circle arcs. The circles containing these arcs are all centered at the origin and are numbered from 1 to  $\infty$ . The  $n$ -th circle has a radius  $R_n$ . We assume  $0 < R_1 < R_2 < \dots$  to take the fact that there are nearby and more distant obstacles into account. In the basic model described here, at the first cascade iteration (stage number  $n = 1$ ), if some first stage blockages exist, they occupy half the angular domain, e.g.,  $[0, \pi]$  or  $[\pi, 2\pi]$  on the circle with radius  $R_1$ . At stage  $n = 2$ , each potential blockage interval of stage  $n = 1$  is divided into two equal length subintervals, and as for stage 1, obstacles of stage 2 can be present and then occupy some of these subintervals, i.e.,  $[0, \pi/2]$ ,  $[\pi/2, \pi]$ ,  $[\pi, 3\pi/2]$ , and  $[3\pi/2, 2\pi]$ . This goes on with stage 3, and so on. An instance of such a random collection of obstacles is depicted in Fig.1. This leads to an organization of obstacles as an infinite binary tree, with the obstacles of stage  $n$  being located on the  $n$ -th circle. Except for the root, each node in this tree is either unblocked (absence) or blocked (presence of an obstacle on the arc in question).

TABLE I: System Model Parameters

Notation	Description
$\Phi, \lambda$	BSs PPP with intensity $\lambda$
$R, R_n$	network parameter and radius of $n$ -th stage
$p, q$	blockage prob. and non-blockage prob.
$N$	max. stage number
$h_x, h^i$	Rayleigh fading of BS $x$ and $i$ -th beam
$K$	blockage penetration loss factor, $K \leq 1$
$I_n$	total interf. in $n$ -th stage
$I_{n, \text{semi}}$	total interf. of semi-indep. model in $n$ -th stage
$I_{n, \text{rep}}$	total interf. of repulsive model in $n$ -th stage
$I_n^l$	total interf. in $n$ -th stage inside beam $l$
$A_n(V)$	local interf. in $n$ -th stage with vol. $V$
$\mathcal{A}_n(s, V)$	LT of local interf. in $n$ -th stage with vol. $V$
$k$	$2^k$ is beam number or UE antenna number

Whether one of the subintervals of the  $n$ -th stage is blocked or not depends on the scenario. A simple model is that where each subinterval is declared blocked randomly and independently with some given probability capturing the angular density of obstacles. Another natural model is that where obstacles are displayed in a periodic manner on each circle. There is a rich variety of such models beyond this first dichotomy (random versus periodic). One can vary the sequence of radii. One can also consider other schemes than this binary one.

In the sequel, by a *box*, we mean any annular region delimited by two adjacent circles and two potential blockage arcs on these circles. An instance of such a box is the annular region ABCD in Fig.1.

Below we first focus on the basic model with this binary subdivision for simplicity. In order to make the analysis easier, we will also assume the  $R_n$  are chosen in such a way that the area of each box is equal for each stage. This requires that

$$R_{n+1}^2 = R_n^2 + 2^n R^2, \quad n \geq 1, \quad (1)$$

with  $R_1 = R$ , an arbitrarily chosen positive constant. Hence, the radius of  $n$ -th stage is set to  $R_n = R\sqrt{2^n - 1}$ . In particular, we set  $R_0 = 0$ .

### B. Network Model

Consider the downlink of an interference-limited cellular network. In this blockage environment, BSs are assumed to be deployed as a homogeneous Poisson Point Process (PPP)  $\Phi$  with intensity  $\lambda$  in  $\mathbb{R}^2$ . Each BS is assumed to have unit transmission power. The typical user is assumed to be located at the origin. The idea being that the radial structure that it sees is a snapshot of its current obstacle environment. Its terminal is first assumed here to have an omnidirectional reception antenna. The case of a terminal with several panels and beam-forming functionalities will be discussed in the forthcoming sections. Each link between a BS and the typical user suffers from independent and identically distributed (i.i.d.) Rayleigh fades  $h_x$ , ( $x \in \Phi$ ), namely the signal power is multiplied by a random variable with an  $Exp(1)$  distribution. The large

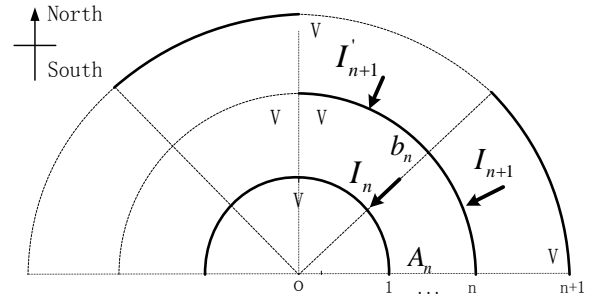


Fig. 2: An illustration of interference relation between adjacent stages.

scale path-loss is neglected throughout. This simplification is justified by the fact that the loss caused by the blockages dominates.

All blockages are assumed to have the same penetration loss denoted by  $K$ , ( $K \in [0, 1)$ ). Let us stress that there is no problem extending the framework described below to the case where this constant is replaced by an independent random variable with support in  $[0, 1]$ . Under the above assumptions, all boxes at all stages have the same volume  $V = \pi R^2/2$ . In the basic independent model, each subinterval is independently blocked with probability  $p$ , ( $p \in (0, 1]$ ) in case of a finite stage blockage environment. In case of an infinite stage blockage environment, we assume that  $p > \frac{1}{2}$  in order to guarantee the finiteness (and integrability of the Light-Of-Sight (LOS) region).

Since blockages are symmetric in law with respect to the  $x$  axis, the analysis will focus on the blockages on the upper half of the plane, as shown in Fig.2.

## III. INTERFERENCE AND COVERAGE

### A. Distribution of Total Interference

The total interference seen by the typical user is

$$J = \sum_{x \in \Phi} h_x K^{N_x}, \quad (2)$$

where  $N_x$  denotes the total number of blockages between the origin and the BS at position  $x$ .

Let  $A(V)$  be the interference created by (and in) a box of volume  $V$ . The Laplace transform of  $A(V)$  is

$$\begin{aligned} \mathcal{A}(s, V) &:= \mathbb{E} \left[ e^{-sA(V)} \right] = \sum_{k=0}^{\infty} (\lambda V)^k e^{-\lambda V} F^k(s) / k! \\ &= \exp(-\lambda V(1 - F(s))), \end{aligned} \quad (3)$$

where  $F(s)$  is the Laplace transform of Rayleigh fading with parameter one, i.e.,  $F(s) = 1/(1 + s)$ .

Consider a box of the  $n$ -th stage, namely between circles  $n-1$  and  $n$ ,  $n \geq 1$ , and with angular stretch  $[\theta, \theta + \frac{2\pi}{n}]$ . Let  $I_n$  be the total interference seen in this box and stemming from the region  $\mathbb{R}^2 \setminus B(0, R_{n-1}) \cap C(0, [\theta, \theta + \frac{2\pi}{n}])$ , with  $B(0, r)$  the ball of center 0 and radius  $r$  and  $C(0, [\phi, \psi])$  the cone of apex 0 and angle  $[\phi, \psi]$ . In other words,  $I_n$  consists of the sum of two terms: (a) the interference coming incurred in this box from the regions at distance more than  $R_n$  from the origin and in the angular interval  $[\theta, \theta + \frac{2\pi}{n}]$ , and (b) the

interference  $A_n(V)$  created and incurred in this very box, as shown in Fig.2. It should be clear that for all such boxes,  $I_n$  has the same distributions as  $I_1$  (this follows from the fact that each is built in the same stochastic way from a binary tree and from the fact that all boxes have the same volume). Hence, in particular,

$$I_1 = (I_2 + I_2')K^{b_1} + A_1(V), \quad (4)$$

where the random variables  $(I_2, I_2', A_1(V))$  are independent and  $I_1, I_2$ , and  $I_2'$  have the same distribution. In addition,  $b_1 \in \{0, 1\}$  is a Bernoulli random variable which equals 1 with probability  $p$  and 0 with probability  $q = 1 - p$ , and is independent of  $(I_2, I_2', A_1(V))$ . Hence, the Laplace transform of  $I := I_1$  satisfies the functional equation

$$\begin{aligned} \mathcal{L}_I(s) &= \mathbb{E}[e^{-sI_1}] \\ &= \mathbb{E}[e^{-sI_2K^{b_1} - sI_2'K^{b_1}}] \mathbb{E}[e^{-sA_1(V)}] \\ &= (p\mathbb{E}[e^{-KsI_2 - KsI_2'}] + q\mathbb{E}[e^{-sI_2 - sI_2'}]) \mathcal{A}(s, V) \\ &= (p\mathcal{L}_I(Ks)^2 + q\mathcal{L}_I(s)^2) \mathcal{A}(s, V). \end{aligned} \quad (5)$$

The total interference received at the typical user is  $\mathcal{L}_I(s) = \mathcal{L}_I(s)^2$  due to the symmetric blockage and BS distributions in the northern and southern  $\mathbb{R}^2$  half-planes, plus independence.

Here is a natural iterative scheme for solving the last functional equation:  $Q^{(0)}(s) = \mathcal{A}(s, V)$  and for all  $n \geq 0$ ,

$$Q^{(n+1)}(s) = (pQ^{(n)}(Ks)^2 + qQ^{(n)}(s)^2) \mathcal{A}(s, V). \quad (6)$$

The distribution of  $I_1$  is that with Laplace transform  $Q^{(\infty)}(s)$ .

It is easy to extend this approach to a finite domain (cascade) case. Assume there are only  $N$  circles. Then the Laplace transform  $M^{(N)}(s)$  of  $I_N$  is equal to  $\mathcal{A}(s, V)$  and more generally, the Laplace transform  $M_n$  of  $I_n$ ,  $1 \leq n < N$  is obtained by

$$M^{(n)}(s) = (pM^{(n+1)}(Ks)^2 + qM^{(n+1)}(s)^2) \mathcal{A}(s, V). \quad (7)$$

Note again that there is no need to assume that  $p > 1/2$  in the finite service area case. This is only needed in the infinite case to guarantee that the total LOS interference be finite.

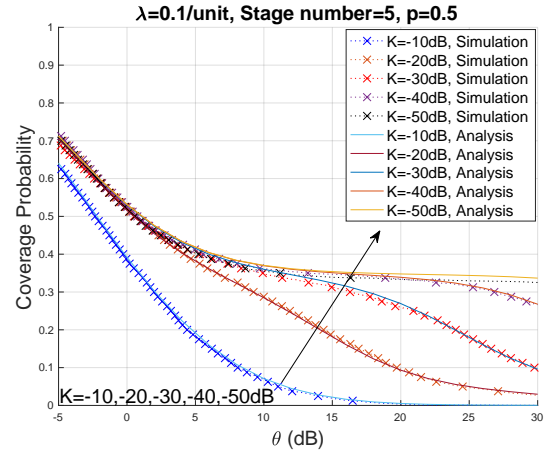
Note that the complexity (number of operations) of this algorithm is linear in  $N$ . For the infinite domain case, an approximation of depth  $n$  has a complexity which is linear in  $n$ .

Ler  $G$  and  $h$  respectively denote the antenna gain and the Rayleigh fading of parameter 1 of the serving BS. Since we assume unit transmission power, the probability of  $\theta$ -coverage (defined as the probability that the SIR exceeds  $\theta$ ) by this BS is

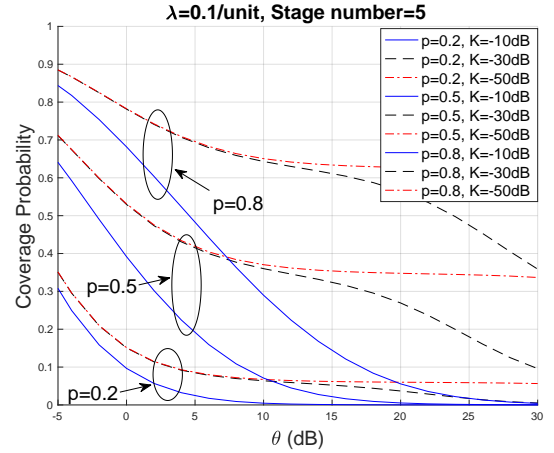
$$P_{\text{cov}}(\theta) = \mathbb{P}\left\{\frac{Gh}{I} \geq \theta\right\} = \mathbb{E}[e^{-\theta I/G}] = \mathcal{L}_I\left(\frac{\theta}{G}\right). \quad (8)$$

## B. Simulation Results

We now assume that a virtual LOS serving BS of the typical user is added to  $\Phi$ , which only suffers from Rayleigh fading. The knowledge of the distribution of interference allows one



(a)  $K$  variations



(b) Sparse/moderate/dense networks

Fig. 3: Coverage performance comparisons in the basic model ( $\lambda = 0.1/\text{unit}$ , max. stage no.  $N = 5$ .)

to get a simple formula for the probability of coverage for a threshold  $\theta$ , which is the probability that the SIR exceeds  $\theta$ .

In Fig.3a, we compare the coverage probabilities of different penetration losses under the virtual BS association in an interference-limited network. Obviously, a higher penetration loss reduces Non-LOS (NLOS) interference from boxes and gives rise to a higher coverage probability. When  $K < -40\text{dB}$ , the interference variations due to different blockage penetration losses is negligible for  $\theta < 25\text{dB}$ .

Fig.3b compares the coverage probabilities of sparse ( $p = 0.2$ ), moderate ( $p = 0.5$ ) and dense ( $p = 0.8$ ) blockage scenarios when the penetration loss  $K$  varies from  $-10\text{dB}$  to  $-50\text{dB}$ . As expected, the coverage probability gaps between different  $K$  cases are very small for sparse blockage scenarios, but not negligible for dense ones. This is in line with the intuition that fewer blockages lead to smaller variations. In addition, the sparse blockage scenario has lower coverage probabilities than the other scenarios, because fewer blockages make sparse scenarios more vulnerable to LOS interference and lead to lower SIR. Finally, the dense blockage scenario is more sensitive to the threshold  $\theta$  due to the higher SIR induced by more blockages.

## IV. VARIANTS OF THE BASIC CASCADE MODEL

## A. A Less Correlated Cascade Model

The basic cascade model can be adapted to represent a less correlated blockage scenario. We construct a new cascade model by independently setting each half of an interval of the basic model to be a blockage or non-blockage state. This variant corresponds to scenarios where blockage sizes are smaller than those in the basic model and it hence exhibits more randomness, since it has more blockage location freedom in each stage. We denote the interference observed by the typical user in this less correlated model by  $\mathcal{L}_{J,lc}$ . In this model, the volume  $V$  that was used in the basic model has to be replaced by  $\tilde{V} \triangleq V/2$ . Let  $\mathcal{L}_{\tilde{I}_1}$  be the interference at the origin due to the quarter plane  $[0, \pi/2]$ . We have  $\mathcal{L}_{J,lc} = \mathcal{L}_{\tilde{I}_1}^4$ . Let  $\tilde{I}_n$  denote the total interference seen in the box in the  $n$ -th stage and stemming from the region  $\mathbb{R}^2 \setminus B(0, R_{n-1}) \cap C(0, [\theta, \theta + \frac{2\pi}{2^{n+1}}])$ . By the same arguments as above

$$\tilde{I}_n = \tilde{I}_{n+1} K^{b_n} + \tilde{I}'_{n+1} K^{b_n} + A_n(\tilde{V}), \quad (9)$$

where  $b_n \in \{0, 1\}$ , ( $\forall n \in \mathbb{N}$ ) represent the presence of blockage in the subinterval. Then, by the same arguments as above,

$$\mathcal{L}_{\tilde{I}_n}(s) = \left( p\mathcal{L}_{\tilde{I}_{n+1}}(Ks)^2 + q\mathcal{L}_{\tilde{I}'_{n+1}}(s)^2 \right) \mathcal{A}(s, \tilde{V}). \quad (10)$$

**Lemma 1:** The basic cascade model has larger Laplace transform of total interference, thereby higher coverage probability, than the less correlated model.

*Proof:* We first prove this by for the model with  $N$  stages. We have

$$\mathcal{L}_{\tilde{I}_N}(s)^2 = \mathcal{L}_{I_N}(s) = \mathcal{A}(s, \tilde{V})^2 = \mathcal{A}(s, V).$$

Take as induction assumption that

$$\mathcal{L}_{\tilde{I}_{N-k}}(s)^2 \leq \mathcal{L}_{I_{N-k}}(s).$$

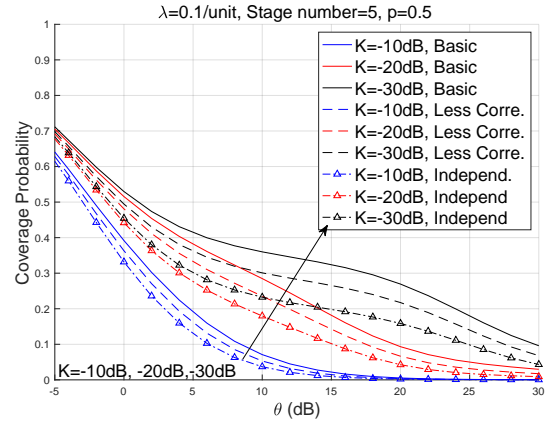
Then

$$\begin{aligned} \mathcal{L}_{\tilde{I}_{N-k-1}}(s)^2 &= \left( p\mathcal{L}_{\tilde{I}_{N-k}}(Ks)^2 + q\mathcal{L}_{\tilde{I}'_{N-k}}(s)^2 \right)^2 \mathcal{A}(s, \tilde{V})^2 \\ &= \left( p\mathcal{L}_{\tilde{I}_{N-k}}(Ks)^2 + q\mathcal{L}_{\tilde{I}'_{N-k}}(s)^2 \right)^2 \mathcal{A}(s, V) \\ &\leq \left( p\mathcal{L}_{I_{N-k}}(Ks) + q\mathcal{L}_{I_{N-k}}(s) \right)^2 \mathcal{A}(s, V) \\ &\leq \left( p\mathcal{L}_{I_{N-k}}(Ks)^2 + q\mathcal{L}_{I_{N-k}}(s)^2 \right) \mathcal{A}(s, V) \\ &= \mathcal{L}_{I_{N-k-1}}(s), \end{aligned}$$

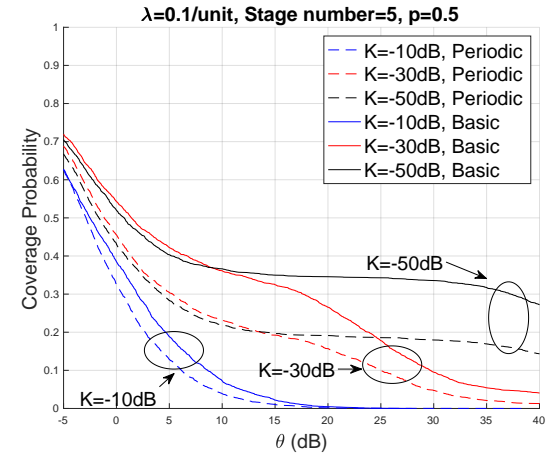
where the first inequality is due to the induction assumption and the second to convexity.

The result for the infinite cascade model is then obtained when letting  $N$  to infinity.  $\square$

In Fig.4a, the coverage probabilities of the two cascade models are plotted when the virtual BS model is assumed. The basic model has higher performance gains under all kinds of penetration losses, especially when  $K$  is very small. It also implies that the Shannon capacity of the basic model, which is a monotonic increasing function of coverage probability, is higher than that of the less correlated model. This is yet



(a) Basic vs. Less correlated Models



(b) Basic vs. Periodic Models

 Fig. 4: Coverage performance comparisons ( $\lambda = 0.1/\text{unit}$ , max. stage no.  $N = 5$ )

another illustration of the principle stated in [8] that the positive correlation created by obstacle shadowing is *beneficial* to wireless communications.

## B. Periodic Cascade Model

The basic model can be revised to emulate well-planned areas such as residential areas/business centers. One of the two subintervals is declared as a blockage randomly and the next subinterval is designated as the non-blockage. This leads to a periodic model with a probability for an interval to be blocked equal to  $1/2$ . This model is only studied here in the finite  $N$  case.

The iterative algorithm for the Laplace transform of interference at the  $n$ -th stage  $I_{n,per}$  is

$$\begin{aligned} \mathcal{L}_{I_{n,per}}(s) &= \mathbb{E}[e^{-sI_{n,per}}] \\ &= \mathcal{L}_{I_{n+1,per}}(Ks)\mathcal{L}_{I_{n+1,per}}(s)\mathcal{A}(s, V). \end{aligned} \quad (11)$$

Fig.4b shows the coverage performance of the two models. The basic model has significant coverage performance gains compared to the periodic one, especially so at high penetration losses.

### C. Independent Model

The independent blockage model [4] is that where each link between the typical user and a BS suffers from an *independent* blockage penetration loss with a distribution that depends on the distance between them. In the present situation, this distribution can be evaluated as follows. For a BS at distance  $r$  from the origin, let  $n(r)$  be the integer such that  $n(r) \leq r < n(r) + 1$ . Using the fact that there are  $n(r)$  potential obstacles between the BS and the origin, which are independently open or closed, we get that the blockage penetration loss  $S(r)$  is a random variable with support on  $\{1, K, K^2, \dots, K^{n(r)}\}$  and such that

$$\mathbb{P}[S(r) = K^l] = \binom{n(r)}{l} p^l q^{n(r)-l}, \quad l = 0, \dots, n(r). \quad (12)$$

In this independent model, the interference at the origin is the Poisson shot-noise

$$I_{\text{ind}} = \sum_{X_i \in \Phi} h_i S_i.$$

Here  $\Phi$  is the BS Poisson PP, the random variables  $h_i$  are independent Rayleigh fades with mean 1, whereas the random variables  $S_i$  is conditionally independent (given  $\Phi$  and  $h = \{h_i\}$ ), and such that  $S_i$  is distributed like  $S(r_i)$  with  $r_i = \|X_i\|$ . By standard arguments,

$$\mathbb{E}[\exp(-sI_{\text{ind}})] = \exp\left(-\lambda 2\pi \int_0^\infty \left(1 - \mathbb{E}\left[\frac{1}{1 + sS(r)}\right]\right) r dr\right), \quad (13)$$

with  $S(r)$  the random variable defined above. Hence

$$\mathbb{E}[\exp(-sI_{\text{ind}})] = \exp\left(-\lambda 2\pi \int_0^\infty \left(1 - \sum_{l=0}^{n(r)} \binom{n(r)}{l} p^l q^{n(r)-l} \frac{1}{1 + sK^l}\right) r dr\right). \quad (14)$$

The probability of coverage under this independent model is then easily deduced from this expression.

## V. BEAMFORMING IN UE - BEST BEAM SELECTION

### A. Motivation

Up to this point in the paper, it was assumed that all UEs are omnidirectional. This section and the next are focused on the case where UEs are equipped with one or more panels, and where each panel has beamforming functionalities. Such a scenario will become a reality in a few years, particularly so in the millimeter wave (mmWave) case. In this setting, panel switch and beam selection/switch will become a particularly important matter as this will allow the network to compensate for the severe path loss in these bands. However, this will require both sides to perform exhaustive sweeping through all possible beamforming directions until the UE steers its beam bore-sight toward the best serving BS's transmission beam. This search procedure is a part of initial access [9] [10] [11] [12] [13] [14] [15]. This beam pairing procedure will be re-initiated in case of severe blockage or UE/BS mobility. It can be refined by hierarchical search (combining both coarse-grained sector and beam refinement phases) or

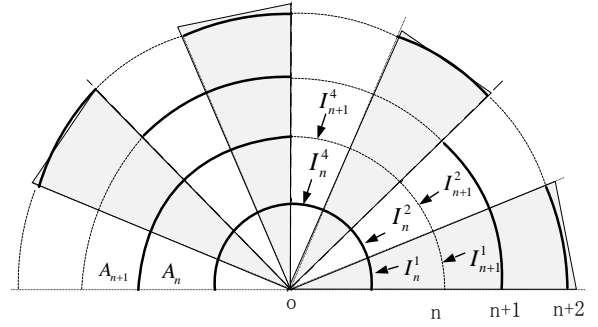


Fig. 5: An illustration of sectorized beam patterns in the cascade blockage model.

omni-directionally reception [10] to shorten the association procedure duration.

There is a large corpus of prior work on the combination of these network paradigms with beamforming in different blockage scenarios and for different link techniques. Unfortunately, none of these capture the impact of correlated blockage on beam selection and beam switching.

Here are interesting and to the best of our knowledge unresolved questions: (a) What is the effect of blockage/shadowing correlation on beam selection? (b) What is the coverage probability under the best beam or the best beam pair policy? (c) What are the performance improvements after a beam switch caused by some blockage event in such a correlated blockage environment?

In the following, we leverage our cascade blockage model to study these questions.

### B. Beamforming Model for UE

The scenario retained for analyzing the case where UEs have a beamforming capability is based on the following assumptions:

- The UE is equipped with  $2^k$  beams, with  $k \geq 1$ .
- The gain in the main lobe of a given beam is a constant  $G \approx 2^k$  with beamwidth  $2\pi/2^k$ . That is, the actual beam pattern is approximated by an ideal sector pattern, as depicted by the shaded areas of Fig.5. On the uplink, all radiated power is hence assumed to be concentrated in the main lobe, whereas on the downlink, when activating beam  $l$ , then only the BSs located in this beam interfere with the serving BS signal.
- Whatever the beam, the serving BS signal on the downlink is still assumed to be provided by an extra virtual BS with power 1 and received with a Rayleigh fading.
- The obstacle structure is the basic binary random model of the last section with obstacles being independently present or absent with probability  $p$  and  $q$  respectively on the arcs  $(\frac{2\pi}{2^n}l, \frac{2\pi}{2^n}(l+1))$ ,  $l = 1, \dots, 2^n$ , of the circle of radius  $R_n$ , for all  $n \geq 1$ . For the same reasons as above, we assume that  $p \geq 1/2$  when considering the infinite obstacle model.
- The UE beams are *in phase* with the obstacle structure. Namely, the beam sectors are respectively on the arcs  $(\frac{2\pi}{2^k}l, \frac{2\pi}{2^k}(l+1))$ ,  $l = 1, \dots, 2^k$ .

Some of these assumptions are debatable. The last one for instance is rather specific and a random phase of one structure w.r.t. the other would be more natural. All these assumptions aim at making the mathematical model as tractable as possible. The extension to less specific scenarios will be considered in subsequent papers.

We still focus on the downlink. We adopt the Max SIR beam selection scenario. This means the UE calculates the SIR in each beamforming direction and selects the beam with the maximal SIR. The *best beam* within this setting is hence defined as the beam which has the maximal SIR among all  $2^k$  beams.

### C. Joint Distribution of Sector Interference

In this subsection  $k$  is a fixed parameter. The UE is assumed to be equipped with  $2^k$  beam sectors. Under the assumptions listed above, let  $I_n^l$  denote the interference received by the UE in beam  $l = 1, \dots, 2^k$  and stemming from the complement of the closed ball of radius  $R_{n-1}$ . Below, we first give iterative formulas allowing one to evaluate the joint Laplace transforms

$$\mathcal{L}_n(s_1, \dots, s_{2^k}) := \mathbb{E} \left[ \exp \left( -s_1 I_n^1 - \dots - s_{2^k} I_n^{2^k} \right) \right], \quad (15)$$

for all  $n \geq 0$ , and all  $(s_1, \dots, s_{2^k})$  in  $\mathbb{R}_+^{2^k}$ . We then show that the coverage probability achieved by the best SIR beam strategy (and other strategies as well) can be derived from the knowledge of  $\mathcal{L}_1(s_1, \dots, s_{2^k})$ .

We build a family of functions  $H_k, H_{k-1}, \dots, H_1$  by induction. The function  $H_k$  is the function of 1 real variable

$$H_k(s) := \mathbb{E} \left[ \exp \left( -s I_k^1 \right) \right]. \quad (16)$$

Note that, by symmetry, this function is the same for all  $l$ .

The function  $H_{k-1}$  is the function of 2 real variables

$$H_{k-1}(s, t) := \mathbb{E} \left[ \exp \left( -s I_{k-1}^{2^{j-1}} - t I_{k-1}^{2^j} \right) \right], \quad (17)$$

that is the joint Laplace transform of  $(I_{k-1}^{2^{j-1}}, I_{k-1}^{2^j})$  at  $(s, t)$ . This function is again the same for all  $j, (1 \leq j \leq 2^{k-1})$ .

More generally, the function  $H_{k-n}$  is the function of  $2^n$  real variables

$$\begin{aligned} & H_{k-n}(s_1, s_2, \dots, s_{2^n}) \\ & := \mathbb{E} \left[ \exp \left( -s_1 I_{k-n}^{2^{n-1}} - s_2 I_{k-n}^{2^n} - \dots - s_{2^n} I_{k-n}^{2^n} \right) \right]. \end{aligned} \quad (18)$$

By symmetry, this function is the same for all  $j, (1 \leq j \leq 2^{k-n})$ . The independence properties imply that

$$\begin{aligned} \mathcal{L}_k(s_1, \dots, s_{2^k}) &= \prod_{l=1}^{2^k} H_k(s_l), \\ \mathcal{L}_{k-1}(s_1, \dots, s_{2^k}) &= \prod_{j=1}^{2^{k-1}} H_{k-1}(s_{2j-1}, s_{2j}), \end{aligned} \quad (19)$$

and more generally

$$\mathcal{L}_{k-n}(s_1, \dots, s_{2^k})$$

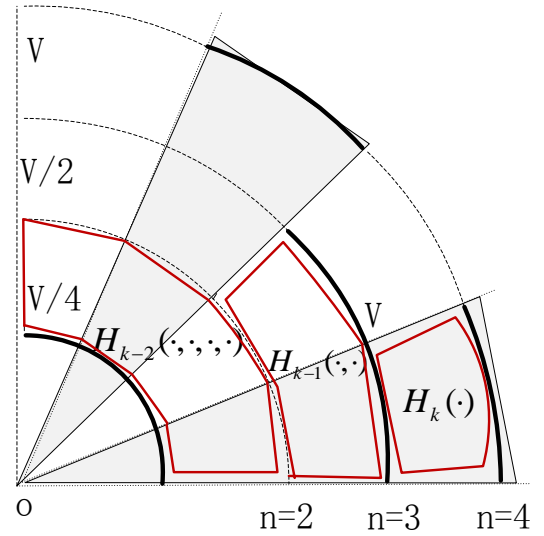


Fig. 6: A pictorial representation of the iteration procedure. The areas enclosed in red are the local boxes involved in  $H_{k-n}(\cdot, \dots, \cdot)$ .

$$\begin{aligned} &= \prod_{j=1}^{2^{k-n}} H_{k-n}(s_{2^n j - 2^n + 1}, s_{2^n j - 2^n + 2}, \dots, s_{2^n j - 1}, s_{2^n j}). \end{aligned} \quad (20)$$

In particular

$$\mathcal{L}_1(s_1, \dots, s_{2^k}) = H_1(s_1, \dots, s_{2^{k-1}}) H_1(s_{2^{k-1}+1}, \dots, s_{2^k}). \quad (21)$$

By the same arguments as in the last section, the function  $H_k(s)$  is the solution of the functional equation

$$H_k(s) = \{pH_k^2(Ks) + qH_k^2(s)\} \mathcal{A}(s, V), \quad (22)$$

which is the analogue of (5). Similarly,  $H_{k-1}(s, t)$  is obtained from  $H_k$  through (see Fig.6)

$$\begin{aligned} H_{k-1}(s, t) &= \\ & \{pH_k(Ks)H_k(Kt) + qH_k(s)H_k(t)\} \mathcal{A}(s, V/2)\mathcal{A}(t, V/2). \end{aligned} \quad (23)$$

More generally, if we know  $H_{k-n+1}$  for some  $1 \leq n < k$ , then  $H_{k-n}$  is obtained from  $H_{k-n+1}$  through

$$\begin{aligned} H_{k-n}(t_1, \dots, t_{2^n}) &= \\ & \{pH_{k-n+1}(Kt_1, \dots, Kt_{2^{n-1}})H_{k-n+1}(Kt_{2^{n-1}+1}, \dots, Kt_{2^n}) \\ & + qH_{k-n+1}(t_1, \dots, t_{2^{n-1}})H_{k-n+1}(t_{2^{n-1}+1}, \dots, t_{2^n})\} \times \\ & \mathcal{A}(t_1, V/2^n) \cdots \mathcal{A}(t_{2^n}, V/2^n). \end{aligned} \quad (24)$$

Note that  $H_{k-n}$  is a function of  $2^n$  variables. So the memory requirement of the iterative associated with (24) is proportional to  $2^k$ . The numbers of function calls required to evaluate in  $H_{k-n}(\cdot, \dots, \cdot)$  is also  $2^n$  (because of the product  $\mathcal{A}(t_1, V/2^n) \cdots \mathcal{A}(t_{2^n}, V/2^n)$ ). Hence the number of operations is also proportional to  $2^k$ , the number of beams.



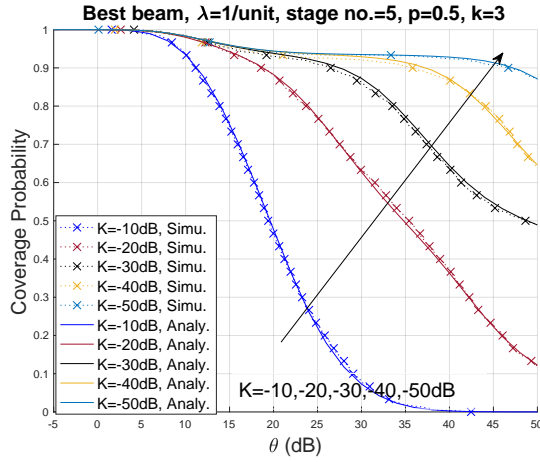


Fig. 7: Best beam selection for different penetration losses  $K$  ( $\lambda = 1/\text{unit}$ , max. stage no.  $N = 5$ ,  $p = 0.5$ ).

#### D. Coverage Probability under Best Beam Selection

Under our assumptions, when denoting by  $h^l$  the Rayleigh fading w.r.t. the BS signal in beam  $l$  and by  $G$  the directional gain, the downlink  $\theta$ -coverage probability of the UE by the best beam is

$$\begin{aligned}
 P_{\text{cov}}^{\text{max}}(\theta) &= 1 - \mathbb{P} \left[ \max_l \left( \frac{Gh^l}{I_1^l} \right) < \theta \right] \\
 &= 1 - \mathbb{P} \left[ \frac{Gh^1}{I_1^1} < \theta, \frac{Gh^2}{I_1^2} < \theta, \dots, \frac{Gh^{2^k}}{I_1^{2^k}} < \theta \right] \\
 &= 1 - \left( \mathbb{E} \prod_{l=1}^{2^k} (1 - e^{-\theta I_1^l / G}) \right) \\
 &= - \sum_{j=1}^{2^k} (-1)^j \\
 &\quad \sum_{1 \leq i_1 < i_2 < \dots < i_j \leq 2^k} \tilde{\mathcal{L}}_1(s_{i_1}, s_{i_2}, \dots, s_{i_j}) \Big|_{s_{i_1}=\theta/G, \dots, s_{i_j}=\theta/G},
 \end{aligned} \tag{25}$$

where  $\tilde{\mathcal{L}}_1(s_{i_1}, s_{i_2}, \dots, s_{i_j})$  stands for  $\mathcal{L}_1$  evaluated at the point  $s = (s_1, \dots, s_{2^k})$  with  $l$ -th coordinate equal to  $s_{i_m}$  for  $l = i_m$  for  $m = 1, \dots, j$ , and 0 elsewhere.

This shows that, as announced, the knowledge of  $\mathcal{L}_1$  allows one to evaluate the probability of coverage under the best beam selection strategy.

#### E. Random Beam Selection Strategy

As a baseline, we also consider a random beam selection strategy where a beam is selected randomly as the serving beam for the typical UE. Since the joint Laplace transform of the interference seen by the origin in the  $2^k$  beams is  $\mathcal{L}_1(s_1, \dots, s_{2^k})$  with  $\mathcal{L}_1$  the function defined in Subsection V-C, the Laplace transform of the interference in any beam is  $\mathcal{L}_1(s, 0, \dots, 0)$ . Hence the coverage probability for SIR threshold  $\theta$  is  $P_{\text{cov}}^{\text{rand}}(\theta) = \mathcal{L}_1(\frac{\theta}{G}, 0, \dots, 0)$ .

#### F. Simulation Results

Fig.7 compares the coverage probability of the best beam scheme for different penetration losses when  $N = 5$ ,  $\lambda = 1$ .

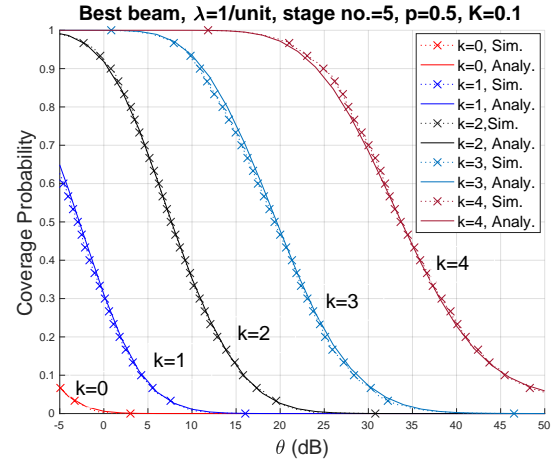


Fig. 8: Best beam coverage performance for different beam numbers. ( $\lambda = 1/\text{unit}$ , max. stage no.  $N = 5$ ,  $p = 0.5$ ,  $K = 0.1$ )

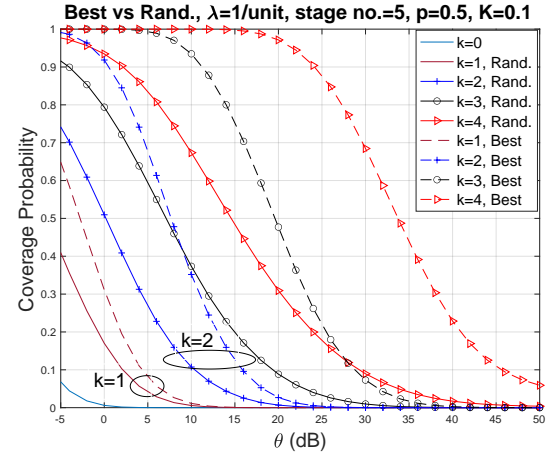


Fig. 9: A comparison between best beam and random beam selections. ( $\lambda = 1/\text{unit}$ , max. stage no.  $N = 5$ ,  $p = 0.5$ ,  $K = 0.1$ )

Our analytical results match well with simulation. As expected, when penetration loss increases, the coverage probability increases due to stronger blockage effects.

The gain of best beam selection are shown in Fig.8 The log in base 2 of the number of beam number varies from  $k = 0$  to  $k = 4$ , and  $K$  is set to 0.1. When  $k = 0$ , the UE is almost uncovered due to strong LOS interference. When  $k$  increases, the coverage probability increases dramatically thanks to higher beam selection diversity, higher directional gain and narrower beamwidth. This in a sense justifies the use beamforming in 5G networks to compensate path loss at mmWave frequencies.

Interestingly, when the number of beams doubles, the gain obtained by the best beam selection over a random beam selection increases as shown in Fig.9. When  $k$  is small, this performance gain is not significant, particularly so at high thresholds, e.g., almost no gain for  $k = 1$ , and a 25% gain for  $k = 2$ , when  $\theta = 10\text{dB}$ . This means when  $k$  is small, a random beam selection does almost as well as best beam selection, at least when the SIR target is high. In contrast,

when  $k$  is large, the beam scanning and selection procedure are justified.

## VI. BEAM SWITCHING IN UE

In this section, we study beam switching. For a static UE equipped with multiple antennas, beam switch could happen for, e.g., the following reasons:

- Deep fade: the current UE beam towards the serving BS suffers from a deep fade, which could not be corrected by conventional physical layer techniques, such as channel coding, interleaving, antenna diversity etc.
- Mobile blockage: the blockages caused by mobile blockers (e.g., a vehicle) could significantly impair the received signal strength and system performance.
- UE rotation: for hand-held devices, the UE is rotated and the current beam is obstructed due to a different holding gesture.

All the above scenarios demand prompt beam switch procedures in order to reduce the outage duration. Since any exhaustive beam sweeping comes with a large delay of synchronization, signal detection, and reference signal quality evaluation for each beam pair, fast association and beam switch procedures are desirable.

A simple procedure is that where the UE operates a switch to a new beam with a given angular separation from the original beam. In this context, it is interesting to investigate the conditional probability that the UE is covered in a target beam conditional on the fact that it is covered (or not covered) in the initial (or source) beam. Without loss of generality, we assume the source beam is the first beam and the target beam is that with index  $l$ . Taking  $l$  close to 1 (mod  $2^k$ ) means a small angular switch, whereas taking it far away from 1 means a large angular switch.

The conditional coverage probability can be obtained from the joint Laplace transform discussed in Section V-C through the relation

$$P_{cov}(\theta, l|\theta, 1) := \frac{\mathbb{P}\{SIR_1 > \theta, SIR_l > \theta\}}{\mathbb{P}\{SIR_1 > \theta\}} = \frac{\mathcal{L}_1(\frac{\theta}{G}, 0, \dots, 0, \frac{\theta}{G}, 0, \dots, 0)}{\mathcal{L}_1(\frac{\theta}{G}, 0, \dots, 0)}, \quad (26)$$

where in the last numerator, the second non-zero argument is for variable  $s_l$ . Other conditional probabilities (like the chance to be covered in the target beam given there is no coverage in the source beam) can easily be deduced from this.

### A. Simulation Results

In Fig.10, for each beam pattern, when the beam index  $l$  increases, the conditional coverage probability degrades as the target beam has more independent blockages. For example, for 16-beam pattern, the 2-th beam has the largest conditional coverage performance because it shares the maximal common blockages with the source one (i.e., the 1-th beam). When beam index increases to 4, only common blockages of the first and second stages are shared by source and target beams. Hence, conditional coverage probability decreases.

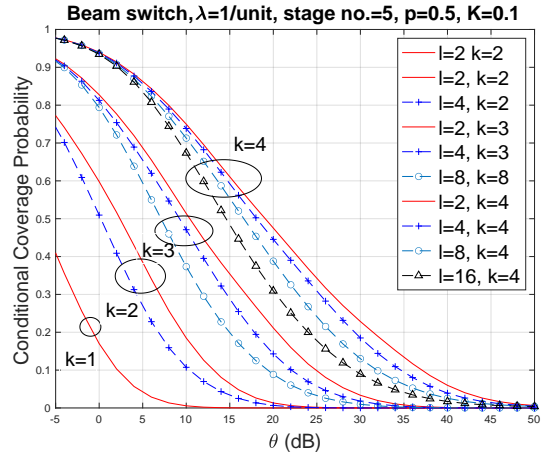


Fig. 10: A comparison of conditional coverage probability of beam switch among different beam patterns. ( $\lambda = 1/unit$ , max. stage no.  $N = 5$ ,  $p = 0.5$ ,  $K = 0.1$ )

When beam index varies from 5 to 8, only first stage blockage is shared by them. When index varies from 9 to 16, target beams have complete independent blockage environments and performance metric achieves the minimum.

### B. Beam Switch Strategy Modification

The above analysis motivates us to modify the classical beam switch strategy for static UEs. In the modified beam switch procedure, the static UE alternatively sweeps beams around the source one, and sequentially increase beam index until a satisfied beam is obtained, instead of sweeping beam towards uni-direction until whole beam space is scanned. This modification takes the advantage of the fact that in the correlated blockage/shadowing environment, the adjacent BSs are often correlated over short space distance/angle [1]. In other words, if a BS has satisfied coverage performance before switch, its nearby BSs are likely to have similar performance, as shown in Fig.10. This fast switch strategy can shorten association duration during beam space scanning.

## VII. CONCLUSION

This paper proposes a multiplicative cascade blockage model to emulate correlated blockage environments. This model is a complement to the Manhattan-type urban model and random blockage models. This model leads to new iterative algorithms for the Laplace transform of interference for omnidirectional UE. Another iterative algorithm is derived to analyze the coverage probability under the best beam selection for beamforming capable UEs. A further analysis of conditional coverage probability shows the benefit of correlation on beam switch. It is also shown that: 1) Sparse blockage environments have inferior coverage performance compared to dense blockage environments. 2) Blockage correlation effects can improve coverage performance in comparison with independent blockage environments. 3) The best beam selection algorithm is very effective for beamforming UEs to compensate path or blockage penetration loss. 5) Correlation brought by blockages can be leveraged to accelerate beam switch and association

procedures. This paper is the first attempt to use multiplicative cascades in blockage effect problem and Rayleigh fading assumption is made for computational tractability. In the future work, other fading models, such as Rician fading or Nakagami fading will be incorporated into this cascade blockage model for more general cases.

### VIII. ACKNOWLEDGEMENTS

The present authors would like to thank Prof. Philippe Martins for suggestions and discussions in preparing this paper.

### REFERENCES

- [1] S. S. Szyszkowicz, H. Yanikomeroglu and J.S. Thompson, "On the Feasibility of Wireless Shadowing Correlation Models", *IEEE Trans. on Veh. Tech.*, vol.59, no.9, pp.4222-4236, Nov.2010
- [2] S. S. Szyszkowicz and H. Yanikomeroglu, "A Simple Approximation of the Aggregate Interference From a Cluster of Many Interferers With Correlated Shadowing", *IEEE Trans. on Wireless Commun.*, vol.13, no.8, pp.4415-4423, Aug. 2014
- [3] M. Taranetz, and M. K. Muller, "A Survey on Modeling Interference and Blockage In Urban Heterogeneous Cellular Networks", *EURASIP J. on Wireless Commun. and Networking*, no.252, pp.1-20, 2016
- [4] T. Bai, R. Vaze, R.W.Heath, "Analysis of Blockage Effects on Urban Cellular Networks", *IEEE Trans. on Wireless Commun.*, vol.13, no.9, pp.5070-5083, Sep. 2014
- [5] M. K. Muller, M. Taranetz and M. Rupp, "Analyzing Wireless Indoor Communications By Blockage Models", *IEEE Access*, vol.5, pp. 2172-2186, 2017.
- [6] F. Baccelli and X. Zhang, "A Correlated Shadowing Model for Urban Wireless Networks", in *Proc. IEEE InfoCom'15*, Hong Kong, China, Apr. 26 -May.1, 2015, pp.801-809.
- [7] J. Lee, X. Zhang and F. Baccelli, "A 3-D Spatial Model for In-Building Wireless Networks With Correlated Shadowing", *IEEE Trans. on Wireless Commun.*, vol.15, no.11, pp.7778-7793, Nov. 2016.
- [8] J. Lee, and F. Baccelli, "On the Effect of Shadowing Correlation on Wireless Network Performance", in *Proc. IEEE InfoCom'18*, Honolulu, HI, USA, 16-19 Apr. 2018
- [9] T. Bai and R. W. Heath, "Coverage and Rate Analysis for Millimeter-Wave Cellular Networks", *IEEE Trans. on Wireless Commun.*, vol.14, no.2, pp.1100-1114, Feb. 2015
- [10] A. Alkhateeb, Y. H. Nam, M. S. Rahman, etc., "Initial Beam Association in Millimeter Wave Cellular Systems: Analysis and Design Insights", *IEEE Trans. on Wireless Commun.*, vol.16, no.5, pp.2807-2821, May. 2017
- [11] J. Fan, L. Han, X. Luo, etc., "Beamwidth Design for Beam Scanning in Millimeter-Wave Cellular Networks", *IEEE Trans. on Veh. Tech.*, vol.69, no.1, pp.1111-1116, Jan. 2020
- [12] H. S. Dhillon, M. Kountouris, and J. G. Andrews, "Downlink MIMO HetNets: Modeling, Ordering Results and Performance Analysis", *IEEE Trans. on Wireless Commun.*, vol.12, no.10, pp.5208-5222, Oct. 2013
- [13] S. M. A. Abarghouyi, B. Makki, M. N. Kenari, etc., "Stochastic Geometry Modeling and Analysis of Finite Millimeter Wave Wireless Network", *IEEE Trans. on Veh. Tech.*, vol.68, no.2, pp.1378-1393, Feb. 2019
- [14] S. S. Kalamkar, F. M. Abinader, F. Baccelli, etc., "Stochastic Geometry-Based Modeling and Analysis of Beam Management in 5G", [Online] Available: <https://arxiv.org/abs/2006.05027>
- [15] M. Giordani, M. Polese, A. Roy, etc., "A Tutorial on Beam Management for 3GPP NR at mmWave Frequencies", *IEEE Commun. Surveys Tuts.*, vol.21, no.1, pp.173-196, 1st Quar. 2019
- [16] R. H. Riedi, M. S. Crouse, V.J.Ribeiro, and R. G. Baraniuk, "A Multifractal Wavelet Model with Application to Network Traffic", *IEEE Trans. on Inf. Theory*, vol.45, no.3, pp.992-1018, Apr. 1999
- [17] J. W. de G. Stenico, L. L. Ling, "Modern Network Traffic Modeling Based on Binomial Multiplicative Cascades", *J. Supercomput.*, Springer, (2015) 71, pp.1712-1735
- [18] F. Baccelli, B. Blaszczyzyn, "Stochastic Geometry and Wireless Networks, Vol. 1", Foundations and Trends in Networking, Now Publisher, 2009, 3:3-4
- [19] I. K. Jain, R. Kumar, and S. S. Panwar, "The Impact of Mobile Blockers on Millimeter Wave Cellular Systems" *IEEE J. Sel. Areas Commun.*, vol.37, no.4, pp.854-868, Apr. 2019
- [20] Y. Li, J. G. Andrews, F. Baccelli, T. D. Novlan, etc., "Design and Analysis of Initial Access in Millimeter Wave Cellular Networks", *IEEE Trans. on Wireless Commun.*, vol.16, no.10, pp.6409-6425, Oct. 2017
- [21] C. Tepedelenlioglu, A. Rajan, and Y. Zhang, "Applications of Stochastic Ordering to Wireless Communications", *IEEE Trans. on Wireless Commun.*, vol.10, no.12, pp.4249-4257, Dec. 2011